Tech Science Press

Resonator Rectenna Design Based on Metamaterials for Low-RF Energy Harvesting

Watcharaphon Naktong[1], Amnoiy Ruengwaree[1,*], Nuchanart Fhafhiem[2] and Piyaporn Krachodnok[3]

[1]Department of Electronics and Telecommunication Engineering, Faculty of Engineering,
Rajamangala University of Technology Thanyaburi (RMUTT), Pathumthani, 12110, Thailand
[2]Department of Telecommunications Engineering, Faculty of Engineering and Architecture,
Rajamangala University of Technology Isan, Nakhon Ratchasima, 30000, Thailand
[3]School of Telecommunication Engineering, Suranaree University of Technology, Nakhonratchasima, 30000, Thailand
[*]Corresponding Author: Amnoiy Ruengwaree. Email: amnoiy.r@en.rmutt.ac.th

Abstract: In this paper, the design of a resonator rectenna, based on metamaterials and capable of harvesting radio-frequency energy at 2.45 GHz to power any low-power devices, is presented. The proposed design uses a simple and inexpensive circuit consisting of a microstrip patch antenna with a mushroom-like electromagnetic band gap (EBG), partially reflective surface (PRS) structure, rectifier circuit, voltage multiplier circuit, and 2.45 GHz Wi-Fi module. The mushroom-like EBG sheet was fabricated on an FR4 substrate surrounding the conventional patch antenna to suppress surface waves so as to enhance the antenna performance. Furthermore, the antenna performance was improved more by utilizing the slotted I-shaped structure as a superstrate called a PRS surface. The enhancement occurred via the reflection of the transmitted power. The proposed rectenna achieved a maximum directive gain of 11.62 dBi covering the industrial, scientific, and medical radio band of 2.40–2.48 GHz. A Wi-Fi 4231 access point transmitted signals in the 2.45 GHz band. The rectenna, located $45°$ anticlockwise relative to the access point, could achieve a maximum power of 0.53 μW. In this study, the rectenna was fully characterized and charged to low-power devices.

Keywords: Metamaterials; energy harvesting; rectenna; Wi-Fi; partially reflective surface; EBG

1 Introduction

Energy is one of the factors that affects human life and helps humans live comfortably. However, energy loss is a significant problem and has a severe impact on the economic and social development of many countries [1]. Today, humans have access to alternative energy sources in various forms, such as water power [2], biomass [3], wind power [4], and solar energy [5]. Another exciting energy source is that generated when an antenna is used as a frequency receiver with a rectifier to convert AC to DC power [6,7]. Radio-frequency (RF) waves are generally spread throughout all regions of a country and is continually used in the form of electromagnetic

waves, such as waves from FM radio, digital television [8], mobile phones [9], and Wi-Fi wireless transmission systems [10]. Several researchers have been interested in improving rectenna system efficiency, as shown in Fig. 1. The development process of such a system can be divided into two main parts.

The first part is the antenna, whereby most researchers have designed the antenna structure with a directional radiation pattern. The advantage of such a radiation pattern is that it can directly receive all of the energy in one direction at the front of the antenna [11]. In collecting energy, antennas with omnidirectional and bidirectional radiation patterns are significantly less effective [12], meaning that the energy obtained is split into several directions.
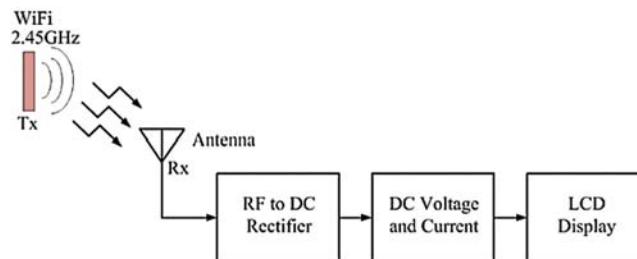
Figure 1: Process of ambient radio-frequency energy harvesting

Therefore, relevant research has focused on combining an antenna with metamaterial of the EBG, which may improve the efficiency of antenna gain. An EBG metamaterial sheet has a multitude of structures according to mathematical shapes, such as rectangles, circles [13], triangles [14], I shapes [15], hexagons, Y shapes, and plus-sign shapes [16]. From this point of view, many researchers have established new structures. Examples of additional research that has been developed include following. (1) The mushroom-like EBG sheet for the installation in an antenna is applied in a square multiple-input–multiple-output (MIMO) system with a combination element that increases from 5.3 to 8.3 dB, a 63.85% rise [17]. (2) A complementary split-ring resonator antenna combined with a square grid structure in a Doppler radar system increased the gain up to 11.3 dB [18]. (3) The gains of a triangular antenna for wireless communication at the low-frequency band of 3.5 GHz and the high frequency band of 5.8 GHz are usually 1.95 and 2.16 dBi, respectively. This gain could be adjusted with an artificial magnetic conductor, which increased the triangular antenna gains to 9.37 and 6.63 dBi, respectively [19]. (4) A rectangular microstrip antenna of 7.45 GHz frequency increased the amplification to 12.31 dBi when combined with a circularly polarized (CP) plate [20]. (5) Researchers developed a structure with metamaterials laid in more than three layers and three dimensions that is called an I-shaped antenna; it is used in 5G applications at the 28 GHz frequency band. When tuned with a dual-band slotted printed circular patch, the maximum gain was 8 dB [21]. (6) A horn antenna used in 5G applications at a low frequency of 2 GHz and a high frequency of 3.5 GHz when tuned with negative-refractive-index metamaterial (NRIM) achieved maximum gains of 8.1 and 8.93 dB, respectively [22]. (7) A 9.5–13 GHz rectangle microstrip antenna, tuned with chessboard polarization conversion metasurface, had a maximum gain of 13.4 dB [23]. (8) A 37.5 GHz rectangle microstrip antenna, tuned with a printed ridge gap waveguide, had a maximum gain of 23.5 dB [24]. (9) The efficiency of a rotated Y-shaped antenna, including a mushroom-like EBG, with a directional radiation pattern, was improved from 89% to 94% by using a slotted EBG ground plane. The antenna gain increased to 8.91 dB at 38.06 GHz for a 5G

cellular communication system [25]. (10) The gain increment was further studied using a 3.6 GHz microstrip patch antenna to install a 4×4 metamaterial surface on the reflector plane layer. The resulting antenna gain of 2.76 dB was enhanced to 6.26 dB when the metamaterial reflector plane was augmented [26]. (11) In addition, the stub tuning technique was used to improve antenna performance [27]. (12) A T-shaped microstrip antenna was designed with three stub shapes. This antenna efficiency could be increased to 52%–72% with a maximum resonance frequency gain of 3.9 dB at 3.25–3.65 GHz for use in future MIMO 5G smartphones and technologies. From all of the aforementioned research, there are advantages in increasing the efficiency of the gain from 4 to 20 dB. However, there are disadvantages in terms of increasing the efficiency of antenna gain, leading to the complexity of the antenna structure. Many tuning steps therefore must be applied to increase antenna gain.

The second development part of an antenna system is focused on electronics circuit design rather than on the antenna structure. A full-wave rectifier circuit and a seven-times-voltage-boosting circuit has been designed. In this design, the system efficiency increases by 18.6% at −50 dBm. The advantage of this approach is that it can increase system efficiency by not requiring the receiver antenna to be 100% energized from the transmitted antenna [28]. This means integrating antennas in one structure with rectifier circuits, which reduce cable losses. The reduction of losses can improve energy converter efficiency by up to 83% at −15 dBm [29]. A wideband stacked patch antenna [30] is composed of a double layer of a substrate to expand bandwidth with parasitic circular patches to increase the directional gain to 6.7 dB. The antenna was designed to connect to a HSMS-2850 rectifier circuit diode. The measured peak efficiency was 63% with an input power of 0 dB. The advantage of a wideband stacked patch antenna is its low profile. However, the gain is low, resulting in a need for high input power. A bridge rectifier circuit design with a harmonic rejection filter was fabricated on a FR4 printed circuit board (PCB) and an interdigital capacitor capable of boosting the power conversion efficiency to 78.7% at 20 dBm with a rectangular double-layer antenna with a gain of 7.3 dB [31]. An antenna designed with a dipole antenna structure using a vapor-conduction technique combined with a coplanar strip-line to help adjust the impedance to suit energy harvesting had an output gain of 8.6 dB. Moreover, an AC-to-DC power converter is essentially a half-wave rectifier.

The DC-bandpass filter used in the present work consists of a Schottky HSMS-2852 high-frequency diode together with a capacitor. This filter acts to protect the power from the microwave to the reflected load, which can convert 83% of the power at −15 dBm [32]. A monopole antenna with square grooving helps adjusts the impedance match between the antenna and the full-wave rectifier circuit to transmit maximum energy. This achieved a gain of 5.6 dB. An output power converter of up to 68% at 5 dBm [33,34] was investigated in a study of a square 2×2 array antenna combined with the technique of adding a fine-tuned I-shaped stub, which resulted in a high gain of 13.4 dB and was able to convert energy up to 77.2% at 21 dBm. Another study examined an I-shaped monopole antenna utilizing the triangular grooving technique on the ground plane and the I-shaped reflector combined with a full-wave rectifier, which resulted in a high gain of 8.36 dB and could convert power up to 40% at 0 dBm [35]. From all of this research, the reviewed antenna structure can increase the gain efficiency. However, there are also disadvantages in the ordinary rectifier circuit, i.e., full- and half-wave rectifiers. The voltage received from the signal is low and it is converted directly into DC voltage energy with no additional voltage gain.

In this research, the two-part development of an RF energy harvesting system from the points of view of its advantages and disadvantages is proposed. The first part is focused on a directional pattern microstrip antenna [11] with an uncomplicated structure that was easy to

adjust and combine with mushroom-like EBG metamaterial [16]. Square structure with a hybrid rectenna [36,37] techniques were applied to increase the gain of the receiver. The second part is to design the RF conversion circuit utilizing a full-wave rectifier circuit [28] combined with a voltage multiplier circuit to increase the voltage. This system uses the designed rectenna to receive energy at a frequency of 2.45 GHz, which is the most widely applied frequency in wireless communication in Thailand. Analysis of the antenna structure and voltage boost circuit design are discussed in Section 2. The effect of antenna design parameters and equipment on the voltage multiplier circuit is discussed in the Section 3. The comparative results of measurement and simulation are discussed in Section 4 regarding the reflective coefficients, electric field plane (E-plane), magnetic field plane (H-plane), antenna gain, and energy capture. Discussion and comparison with previous works are presented in Section 5. Conclusions are drawn in Section 6.

2 Antenna Structural Design and Rectifier Circuits

2.1 Antenna Structural Design

The microstrip antenna structure designed in the present work is a basic rectangle shape, as shown in Fig. 2a, which had the advantage of having an uncomplicated structure. It was easy to design with a few fine-tuning points. The electromagnetic wave was spread in a specific direction to cover the area as needed [11]. The antenna structure was designed and fabricated on a PCB made of FR4 substrate. The advantages of this PCB are the following. The structure is strong and not easily broken; it has the form of a thin sheet and is easily accessible in Thailand. It is generally used to design, develop, and build antennas [11,12]. PCB FR4 substrate maintains constant electrical conductivity throughout the sheet. Therefore, the measurement results were close to actual simulation results. The selected PCB FR4 substrate has a dielectric constant (ε_r) of 4.4, the thickness of the Cu sheet of the antenna (t_{ant}) and the (t_{ground}) is 0.035 mm, and the thickness of the base material (h_{FR4}) is 1.60 mm, as shown in Fig. 2a. The designed antenna structure has a width W as calculated by Eq. (1) and length L as calculated by Eq. (2) [38]. In this paper, the design technique for the optimization gain of square structure microstrip antennas applied to fabricate the antenna was combined with mushroom-like EBG technology [16]. The EBG plate was positioned around the central radiator as a 3 × 3-type array antenna in which the function of the mushroom is to cover the spread of energy on all sides, as shown in Fig. 2b. The g-gap space of the EBG structure can be calculated by Eq. (3) [38]. One writes

$$W = \frac{\lambda}{2}\left(\frac{\varepsilon_r + 1}{2}\right)^{-1/2}, \tag{1}$$

$$L = 0.49\left(\frac{\lambda}{\sqrt{\varepsilon_r}}\right), \tag{2}$$

$$g = L_{EBG} - L_s. \tag{3}$$

Metamaterial with an I-shaped slot structure was chosen to improve the structure of the antenna to increase the gain, as shown in Fig. 3a. The main advantage of this metamaterial structural design is simply to tune the resonance frequency. The unit cell (I-shaped slot) on the metamaterial measured 0.5λ, which provided the best energy transfer. The equivalent circuit of the slot is the series of L and C components, as shown in Fig. 3b. The appreciation of permittivity and permeability is calculated using Eqs. (4) and (5) [38].
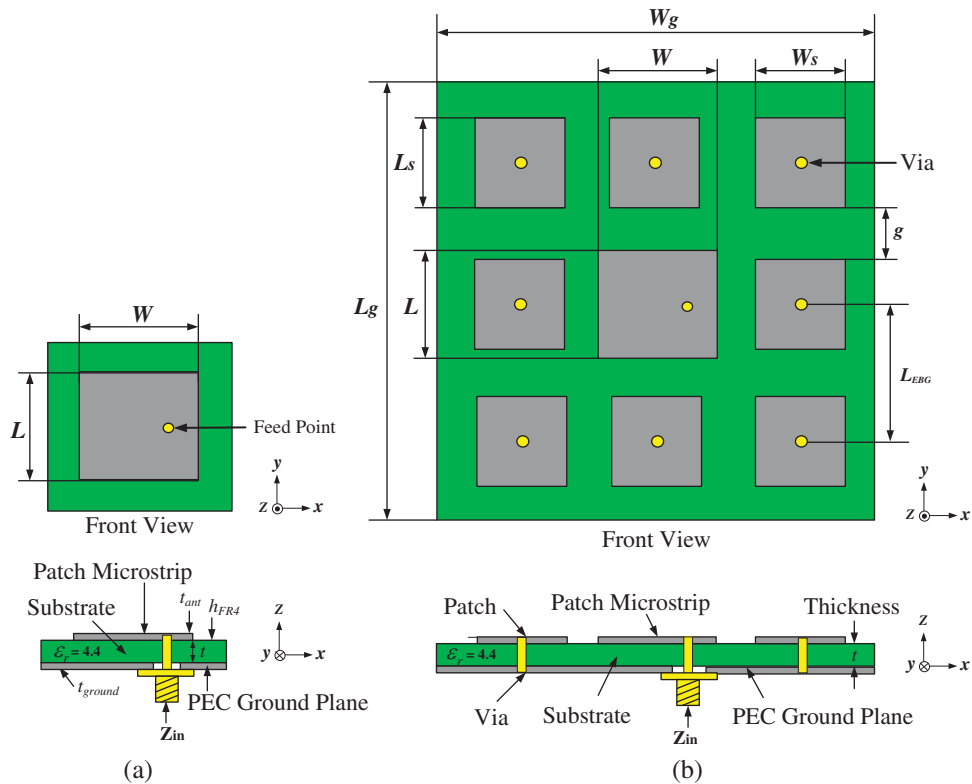
Figure 2: (a) The microstrip antenna structure based on rectangle shape (b) the g-gap space of the EBG structure
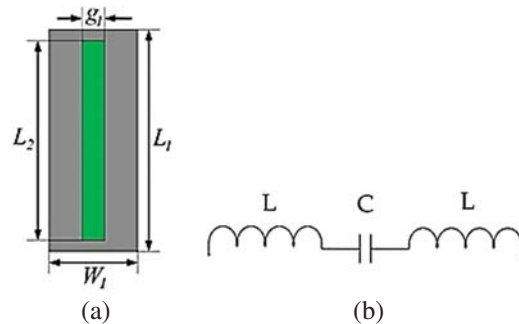
Figure 3: (a) Unit cell of I-shaped slot and (b) equivalent circuit in LC model

The structural design of the metal sheet was done on FR4 substrate. After structural adjustment, the width parameter of the metamaterial W_1 was 15.30 mm (0.0125λ) and the width of the gap g_1 was 3.67 mm (0.031λ). The length value of material L_1 was 61.22 mm (0.5λ). Adjusting the length of the gap, L_2, affected the gain, beginning with the adjustments on the wavelength 0.424$\lambda < L_2 < $ 0.484λ, which were equal to 51.91, 55.71, and 59.26 mm. The most effective tuning was $L_2 = $ 55.71.

Both L_1 and L_2 values had features approaching Mu- and Epsilon-Near-Zero (MENZ), i.e., MENZ material. MENZ is classified into two types. The first type is a negative value approaching

zero, which allows the wave to propagate through the metamaterial structure. The second type is the positive value approaching zero, in which the metamaterial acts as the reflecting surface. In this case, the conditions of permittivity and permeability are positive values that approach zero.

Consequently, this metamaterial structure served as a reflecting surface that partly reflected the waves and partly transmitted waves through it. The metamaterial was designed to be a two-dimensional (2D) wave band gap by combining the antenna structure, as shown in Fig. 4. The height (h) between the radiator and metamaterial sheet can be calculated by Eq. (6):

$$\varepsilon_r \approx \frac{2}{jk_0d}\frac{1-v_1}{1+v_1}, \tag{4}$$

$$\mu_r \approx \frac{2}{jk_0d}\frac{1-v_1}{1+v_1}, \tag{5}$$

where

$v_1 = S_{21} + S_{11},$

$v_2 = S_{21} - S_{11},$

$k_0 = \omega/c,$

and S_{11} is the return loss, S_{21} the mutual coupling, ω the radiation frequency, d the dielectric thickness, and c the speed of light. The aforementioned height is calculated as follows:

$$h = \frac{c}{2f}\left(\frac{\varphi_{PRS} + \varphi_{EBG}}{360°}\right). \tag{6}$$
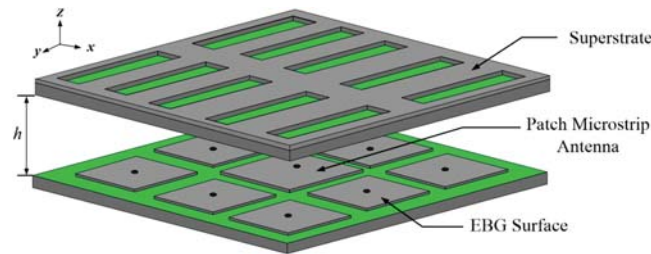
Figure 4: Prototype antenna structure

2.2 Rectifier Circuit

The electrical energy stored from the RF signal of the frequency band of 2.45 GHz is the AC. The full-wave rectifier circuit converts AC to DC, which, in conjunction with the Cockcroft Walton voltage multiplier circuit, increased the voltage. Diode HSMS-2850 [32] is a well-known diode used in voltage multiplier circuits of high-frequency energy-storage systems in which the diodes are attached in bulk to increase the voltage, as shown in Fig. 5. A microcontroller (PIC16F877A) was used as the processing unit to measure and display the rectenna power and voltage values, as shown in Fig. 6a, and a C language program was used to control the LCD screen display (16×2) to show the results. The PIC16F877A microcontroller has the advantage of being able to measure a minimum power of 0.005 μW, which is better for showing on small-scale values than a typical

digital meter. Usually, the efficiency value obtained from the receiver part's power-measurement results can be calculated by the following equation:

$$\eta = \frac{P_{output}}{P_{input}} \times 100. \tag{7}$$
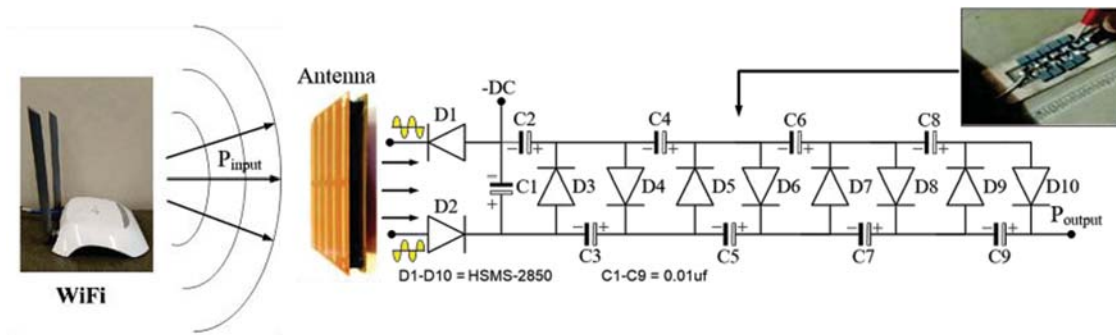
Figure 5: Connection of prototype antenna to rectifier and Cockcroft Walton voltage multiplier circuit

(a)   **(b)**

Figure 6: Rectenna power and voltage meter. (a) PIC16F877A microcontroller, (b) voltage multiplier circuit and LCD

3 Design Results

3.1 Simulation of Antenna Design

First, the design parameters of a rectangular microstrip antenna at 2.45 GHz were calculated using Eqs. (1) and (2), as defined in Fig. 2a. It was found that the width $(W) = 37.54$ mm and length $(L) = 28.93$ mm had S_{11} equal to -12.65 dB, as shown in Fig. 7a. The simulation results of impedance and gain were $49.85 - j20.93 \ \Omega$ and 7.54 dBm, respectively. The design of a mushroom-like EBG with an eight-element square structure to lay around the radiator is shown in Fig. 2b; The mushroom-like EBG parameters could be calculated using the width (W_s) and length (L_s) of 28.46 mm, which was 0.035λ. The shorting post diameter connecting the EBG patch to the ground plane at the via point was 1.46 mm (0.012λ), as shown in Fig. 2b. The model used to find the distance at which to place the EBG patch to obtain the best reflection phase value responded to the 2.45 GHz frequency band, as shown in Fig. 8. At the beginning of the tuning process, the length L_{EBG} (wavelength of $0.245\lambda < L_{EBG} < 0.326\lambda$) was adjusted from 30, 35, and 40 mm, as shown in Fig. 7b. After this tuning, the gains of the prototype antenna with metamaterial were

7.86, 7.91, and 7.74 dB, respectively. These results show that the best reflection phase was achieved at $L_{EBG} = 35$ mm. This value was used to calculate the distance of the gap (g) between the EGB patches, which was found to be $g = 6.54$ mm, and the magnification rate was 7.91 dB. The antenna gain with metamaterial increased by 7.91 dB (4.67%) relative to that without metamaterial (7.54 dB). Eight mushroom-like EBG patches measuring 120 mm^2 × 120 mm^2 in width and length, with shorting posts, were emplaced around the microstrip antenna, as shown in Fig. 2b. By inserting these eight mushroom-like EBG patches, the radiation pattern covered all useful directions. Observation of the electromagnetic near-field distribution resembled a mushroom, as shown in Fig. 7c.
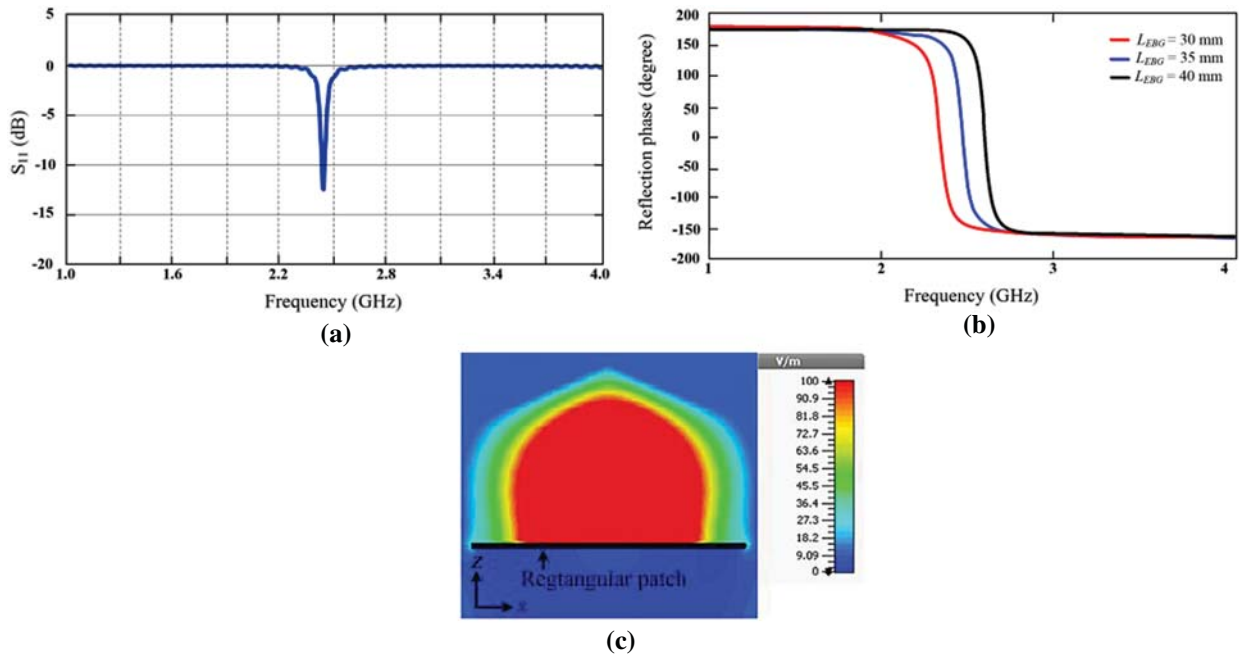
Figure 7: Simulation results of prototype antenna upon addition of eight mushroom-like EBG patches. (a) Reflection coefficient, (b) reflection phase, (c) electromagnetic near-field distribution over prototype antenna

The simulation model of a single unit cell for the slot-shaped metamaterial is shown in Fig. 8. The permeability and permittivity both had a positive value approaching zero, MENZ, with the characteristic that allows waves to propagate; thus, as shown in Fig. 9, this medium acted as a surface that partially reflected the waves and partially transmitted the waves. This type of material provides a 2D electromagnetic frequency gap.

From the design and simulation of the sub-structure sheet structure, as shown in Fig. 2a, the radiator matrix (2 × 5) layout was tested and simulated in transverse-electric (TE) and transverse-magnetic (TM) polarization modes to find the best gain received. The structure of the metal sheet material had the same width and length as the antenna structure, i.e., 120 mm^2 × 120 mm^2, a width of $W_p = 24$ mm (0.196λ), and a length of $L_p = 60$ mm (0.49λ), as shown in Fig. 9.
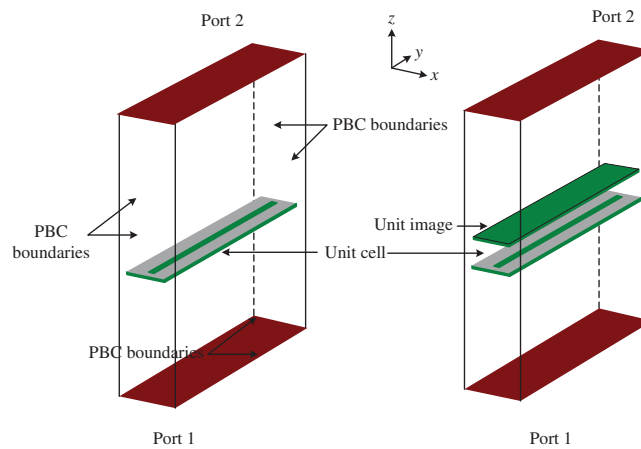
Figure 8: Unit-cell model for slot-shaped metamaterial
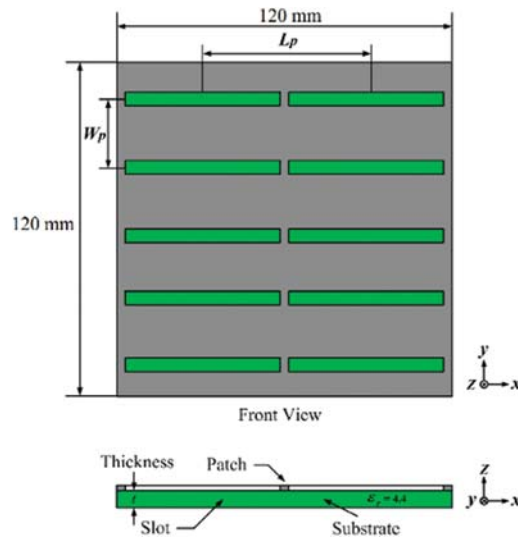
Figure 9: Multiple-cell model for slot-shaped metamaterial

The simulation results for the permittivity (δ) and permeability (μ) at the frequency (1–4 GHz) of the designed structure are shown in Fig. 10. The slot-shaped metamaterial super-strate is classified into MENZ values. Additionally, it can be widely used for many applications for which high-power coherent emission is needed, such as radar, lasers, and antennas. In the work described in this paper, this structure was applied in a resonator antenna performing as the upper layer of a rectangular microstrip antenna. Before designing the resonator antenna, the wave propagation passing through a medium was discussed, as shown in Fig. 11. Whenever the metamaterial became one of the slot-shaped functions, the reflected and refracted waves of propagating electromagnetic waves passing through a medium occurred. In this case, the electromagnetic waves propagated along the x direction. Regarding the polarization modes that can be applied, two polarization modes are possible, as follows.
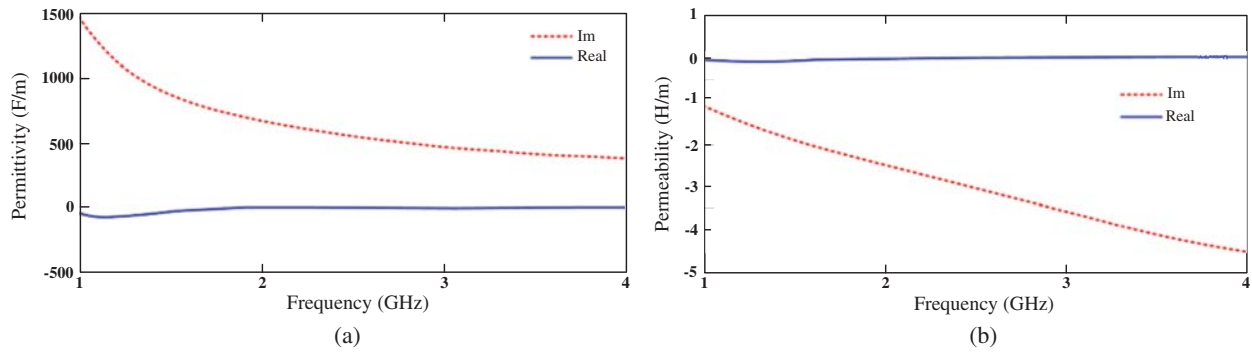
Figure 10: Simulated results of slot-shaped unit. (a) Permittivity (δ), (b) permeability (μ)
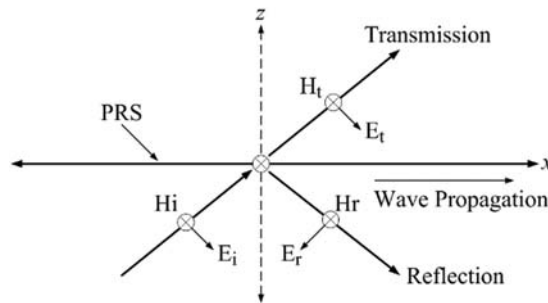
Figure 11: Electromagnetic propagation when passing through a medium

A. TE polarization mode

    Fig. 12a depicts the TE polarization mode. The metamaterial setup based on a slot is depicted along the y axis, so the electromagnetic waves propagate in the x direction. The electric fields of the rectangular microstrip antenna propagate along the y axis. Therefore, the TE polarization mode can have more magnetic fields of transmitted waves than reflected waves, as shown in Fig. 13a.
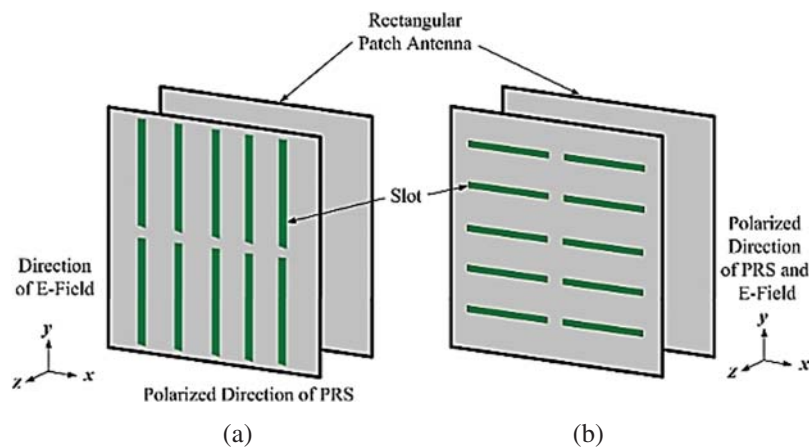
Figure 12: Geometries of resonator antenna. (a) TE, (b) TM
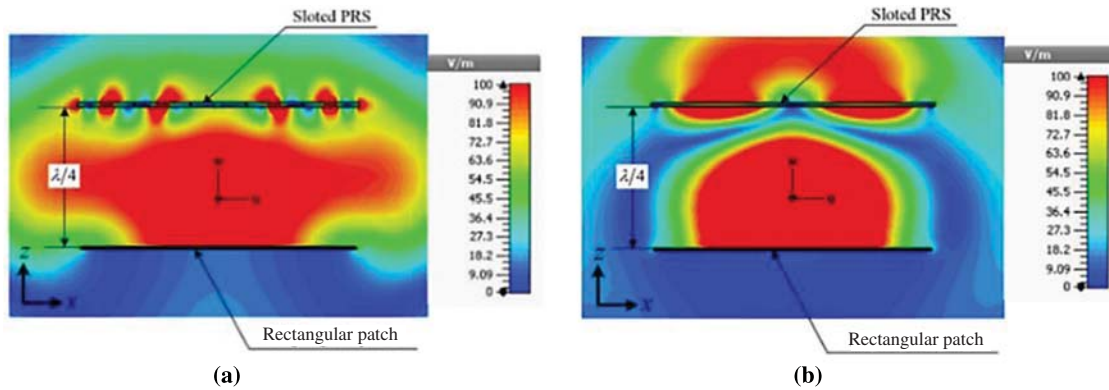
Figure 13: Electric field intensity propagation passing through the medium near-field distributions of proposed TE and TM modes. (a) TE mode, (b) TM mode

B. TM polarization mode

The metamaterial setup based on the slot-shaped structure is along the x axis, so the electromagnetic waves propagate in the y direction. Furthermore, the electric fields of a primary radiator propagate along the y axis. Consequently, the PRS polarization direction has only electric fields in the TM polarization mode, as displayed in Fig. 12b. In this case, the propagation of the transmitted waves can be less than that of the reflected waves, as shown in Fig. 13b.

From the theory explained above, the wave propagation is obstructed by the metamaterials based on the PRS slot-shaped structure along the x and y directions in the TE and TM polarization modes, respectively.

In TE mode, the slot-shaped metamaterials act as the rectangular microstrip superstrate installed on an antenna with a quarter-wavelength dimension in the medium for radiating in phase. Fig. 13a illustrates the near-field distribution of the proposed TE mode. It can be seen that the spread of waves radiating through a slot-shaped superstrate is small. The red area shows the maximum electric field strength from the rectangular patch antenna that could reach only marginally to the top of the metamaterial plate surface due to the impedance mismatch between the antenna and metal plate mounted along the cross-section. The yellow, green, blue, and dark blue areas show the decreasing electric field intensity.

However, as shown in Fig. 13b, the wave propagation of the TM mode can be seen to be radiating very well. It was found that the maximum electric field strength could be exported from the antenna through the top of the metal sheet in the same direction due to the excellent impedance between the antenna and metal plate in the same horizontal direction. c, f, ϕ_{PRS}, and ϕ_{EBG} are the wave velocity, resonant frequency, reflection phase of the PRS, and reflection phase of the EBG, respectively. If the reflection phases of the EBG and PRS are 0° and 155° as plotted in Fig. 14, then the h parameter is 26.36 mm.

Simulation results of the proposed microstrip antenna gain with the EBG and metamaterial sheet are shown upon changing the distance between $0.04\lambda < h < 0.8\lambda$ starting from 5 mm up to 100 mm in increments of 10 mm, indicating that the gain was most affected in the response. From this result, it was found that the best distance was 10 mm, which had the highest gain of 11.97 dB, as shown in Tab. 1, since the distance between the antenna and metal sheet had an

offset angle of 0°. The current density direction is shown in Fig. 15, simulation of the microstrip antenna with the full metal plate (EBG) in Fig. 16, and the best parameters in Tab. 2.

(a)   **(b)**
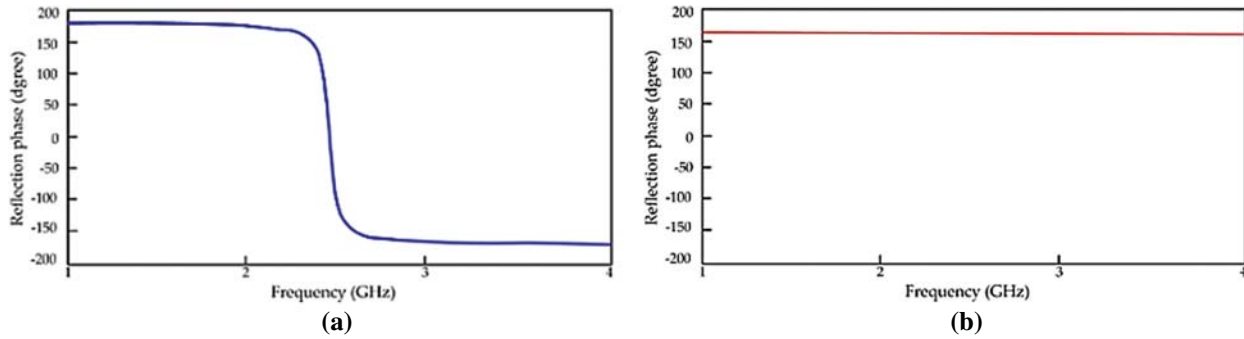
Figure 14: Simulation results of reflection phases of metamaterials. (a) Reflection phase of EBG at 2.45 GHz, (b) reflection phase of PRS at 2.45 GHz

Table 1: Simulation gain results of proposed antenna

Distance between microstrip and metamaterial (mm)	Gain (dB)
5	11.70
10	11.97
20	10.83
30	9.88
40	9.72
50	9.79
60	10.36
70	10.34
80	10.31
90	10.29
100	10.28
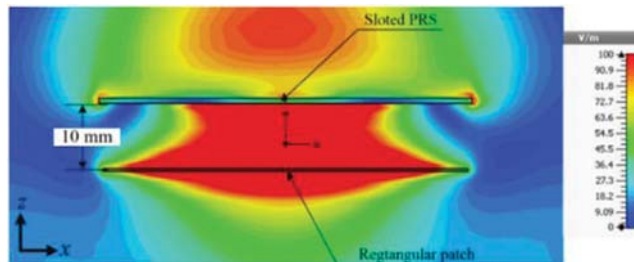
Figure 15: Near-field distributions

(a)   (b)
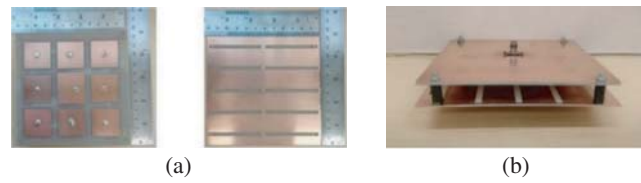
Figure 16: Photographs of proposed antenna. (a) Rectangular microstrip antenna with EBG surface and PRS (b) resonator antenna

Table 2: Parameters of proposed antenna

Parameters	Size (mm)
W: Width of patch microstrip antenna	37.54
W_g: Width of ground plane	120.00
W_s: Width of patch EBG	28.46
W_p: Separation width of slot PRS	24.00
W_1: Width of patch metamaterial	15.30
L: Length of patch microstrip antenna	28.93
L_g: Length of ground plane	120.00
L_s: Length of patch EBG	28.46
L_p: Length of slot PRS	60.00
L_1: Length of patch metamaterial	61.22
L_2: Length of slot metamaterial	55.71
L_{EBG}: Length of patch EBG	35.00
g: Gap between a patch of EBG	6.54
g_1: Gap between a patch of metamaterial	3.67
t_{ant}: Thickness of Cu antenna	0.035
t_{ground}: Thickness of Cu ground	0.035
h_{FR4}: Thickness of FR4	1.60
h: Distance between radiating element and PRS	10.00
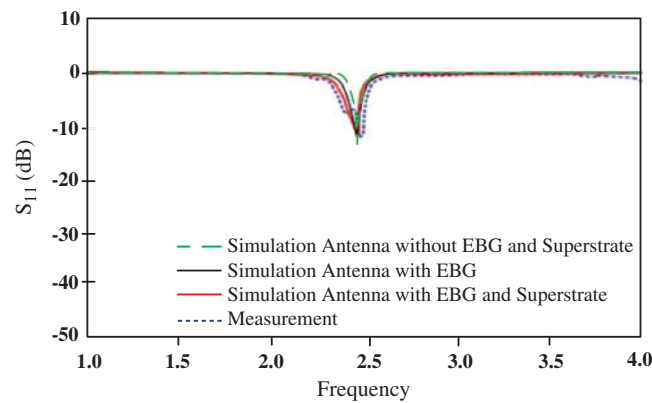
Figure 17: Simulated and measured S_{11} (dB)

The rectangular microstrip antenna prototype is surrounded by a mushroom-liked EBG, which was fabricated using two sides of FR4 sheet with a dielectric constant of 4.3, as shown in Fig. 16a. In addition, the PRS superstrate was located above the radiating element with a spacing of approximately 10 mm, as shown in Fig. 16b. When S_{11} is analyzed as shown in Fig. 17, Tab. 3 illustrates the simulated and measured results for the proposed antenna. The input impedances of simulation and measurement results were close to 50 Ω.

Table 3: Simulated and measured results for antenna based on S_{11} and voltage standing wave ratio (VSWR)

Antenna	S_{11} (dB)	VSWR	Z_{in} (Ω)
Simulation antenna without EBG and superstrate	−13.84	1.59:1	53.85 + j12.05
Simulation antenna with EBG	−12.31	1.63:1	69.24 + j4.99
Simulation antenna with EBG and superstrate	−12.65	1.62:1	49.85 − j20.93
Measurement of proposed antenna	−10.05	1.92:1	47.94 − j25.34

A microstrip antenna was reconstructed from a conventional patch using an EBG surface placed on a similar rectangular patch to improve directional gain from 7.21 to 8.08 dB. Subsequently, when the directional antenna was applied to the resonator antenna by adding the PRS superstrate, the maximum gain increased to 11.97 dB. When the proposed antenna was compared with the patch microstrip antenna, the directional gain efficiency was enhanced to 39.76%. The 3D perspective of the radiation pattern with maximum gain is shown in Fig. 18.
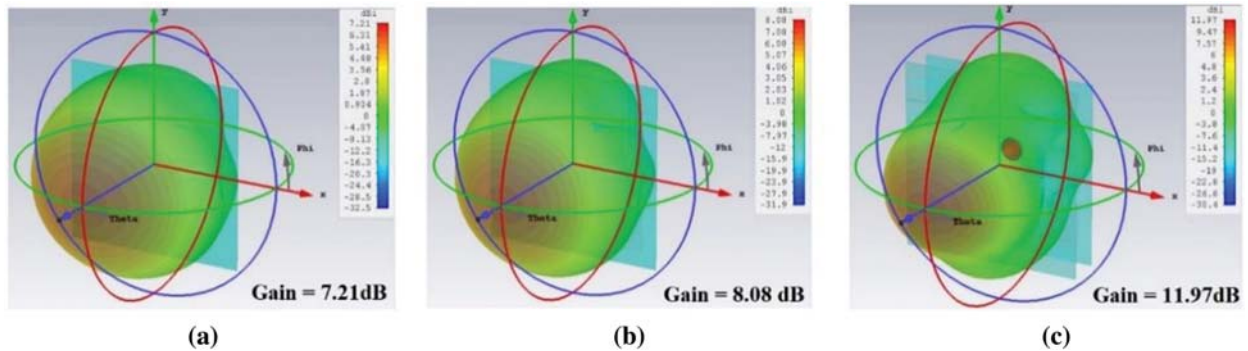
Figure 18: 3D perspectives of radiation pattern with maximum gain: (a) Patch microstrip antenna, (b) patch microstrip antenna surrounded with EBG, and (c) proposed antenna

The results of comparing the measured and simulated gains of the microstrip antenna in Fig. 16 are shown in Tab. 4. These results tend to be in the same direction with the maximum gain of 11.97 dB. The efficiency was increased by 39.76%.

The radiation pattern in the E- and H-planes at a frequency of 2.45 GHz are plotted in Fig. 19. The characteristic of the radiated energy patterns is that of a directional radiation pattern. However, a back lobe perhaps appeared because the resonator antenna reflected and forwarded high-power waves. The half-power beamwidth in the E- and H-planes were 54.6° and 54.5°, respectively.

Table 4: Comparison of measured and simulated gains of various antenna types

Antenna type	Simulated gain (dB)	Measured gain (dB)
Microstrip antenna	7.21	4.75
Microstrip antenna with EBG	8.08	7.19
Proposed antenna	11.97	11.62

(a)   (b)
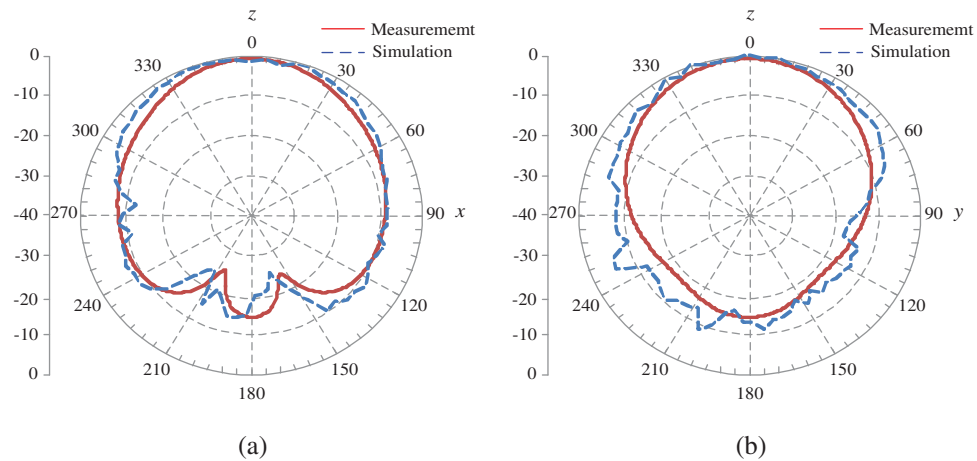
Figure 19: Simulated and measured radiation patterns. (a) E-plane, (b) H-plane

3.2 Rectifier

The DC energy-harvesting measurement from connecting the prototype antenna with the rectifier and voltage multiplier circuits is shown as a block diagram in Fig. 20. The experiment was done with voltage multiplier circuits of 6, 8, 10, and 12 times, tested at 0.6 m, which was the best distance for receiving maximum voltage. It was found from the experimental results that a multiplier circuit of 8 times yielded better performance than that of 6, 10, or 12 times, as shown in Tab. 5.
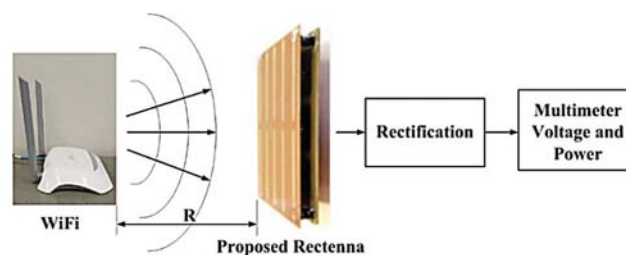
Figure 20: Block diagram of ambient RF energy harvesting

Table 5: Energy-harvesting measurement results

Distance (m)	Measurement results	Voltage multiplier circuits			
		6	8	10	12
0.6	Voltage (mV)	2.23	2.71	2.63	2.59

4 Rectenna System Measurement Results

Experiments were carried out on two parameters for receiving maximum energy: signal receiving distance and direction angle of the Wi-Fi spot and rectenna response. The signal receiving distances were 0.5, 1, 1.5, 2, 2.5, and 3 m, and the direction angles of the Wi-Fi spit and rectenna response were 0°, 15°, 30°, 45°, 60°, 75°, and 90°. The best value was at a distance of 1 m and the direction of 45°. The results were a voltage of 2.82 mV, current of 0.34 mA, and power of 0.95 μW, as shown in Tab. 6. In more than 3 meters measuring distances and the direction angle greater than 90°, the measurement was lower than 0.05 mV/mA, causing the signal meter not to display on the screen. Wi-Fi transmitter was the TP-Link TL-WRB840N, commonly used in Thailand, connected to the directional antenna with the transmitting power of −30.04 dB.

Table 6: Energy harvesting measurement results

Angle	Measurement results	Distance (m)					
		0.5	1	1.5	2	2.5	3
0°	Voltage (mV)	1.64	1.85	1.72	1.56	1.12	0.09
	Current (mA)	0.19	0.21	0.19	0.17	0.10	0.08
	Power (μW)	0.31	0.39	0.32	0.26	0.11	0.007
15°	Voltage (mV)	1.78	1.98	1.74	1.62	1.24	1.17
	Current (mA)	0.20	0.23	0.21	0.15	0.09	0.07
	Power (μW)	0.35	0.45	0.36	0.24	0.11	0.08
30°	Voltage (mV)	2.53	2.80	2.28	1.82	1.34	1.12
	Current (mA)	0.21	0.32	0.21	0.12	0.09	0.08
	Power (μW)	0.53	0.89	0.47	0.21	0.12	0.08
45°	Voltage (mV)	2.54	2.82	2.31	1.97	1.46	1.25
	Current (mA)	0.21	0.34	0.24	0.13	0.09	0.08
	Power (μW)	0.53	0.95	0.55	0.25	0.13	0.10
60°	Voltage (mV)	2.14	2.52	2.23	1.75	1.27	1.16
	Current (mA)	0.20	0.24	0.22	0.18	0.10	0.08
	Power (μW)	0.42	0.60	0.49	0.31	0.12	0.09
75°	Voltage (mV)	2.14	2.52	2.23	1.75	1.27	1.16
	Current (mA)	0.19	0.23	0.19	0.10	0.09	0.07
	Power (μW)	0.40	0.57	0.42	0.17	0.11	0.08
90°	Voltage (mV)	2.01	2.12	1.92	1.68	1.08	1.04
	Current (mA)	0.13	0.18	0.14	0.09	0.07	0.05
	Power (μW)	0.26	0.38	0.26	0.15	0.07	0.05

5 Discussion

The design and construction of a rectenna system using a directional microstrip antenna with an integrated magnetic stripe design (EBG) plate with a multiple voltage circuit were presented. The antenna designed in the present work was compared with those designed in previous works as follows.

In [29], an uncomplicated antenna with a gain of 8.6 dBi for low-energy harvesting at the 2.45 GHz frequency band was designed. The rectenna in [30] consisted of an antenna with a directional gain of 6.7 dB at 2.45 GHz. A rectifier circuit with a HSMS2850 diode achieved low-energy harvesting with an efficiency of 63% when the input power was 0 dBm. The designed antenna matched the rectifying circuit and eliminated unwanted harmonics, resulting in an 83% efficiency when using a 1400-Ω resistor and converting power up to 83% at -15 dBm. This antenna design is not complicated, but has low gain and high power consumption.

A rectifier circuit with four switch diodes and an interdigital capacitor was designed to increase the DC output voltage in another antenna [31] that operated at the 2.45-GHz frequency band to reduce high harmonic values and had a gain of 7.13 dB, resulting in an efficiency of 78.7% when using 4 kΩ impedance with a transmitted signal power of 20 dBm. This antenna is also not complicated, but has low gain and high transmitting power.

Another antenna was designed using square-shaped tuning techniques to tune the impedance bandwidth and increase the maximum gain to 5.6 dB [32]. This antenna is compact, measuring 18 mm $\times$ 30 mm, with an L-shaped impedance-matching network rectifier to allow the input impedance to match that of the antenna. A maximum voltage of 3.24 V was obtained with a load resistance of 5 kΩ. Its maximum efficiency was 75.5% in simulation and 68% as measured with a transmitted power of 5 dBm at 2.45 GHz. This antenna is small and compact, but has low gain and high transmitting power.

In [33], frequency-selective-surface (FSS) sheet structure techniques were used for RF energy harvesting with a geometric shape consisting of a sequence of unit cells. The gain was 9.4 dB when connected with a full-wave rectifier circuit that could convert power up to a conversion rate of 61% at a transmitted power of 15 dBm. The gain and transmitted power are both high, but the structure is complicated.

In [34], a square 2×2 array antenna designed by adding an I-shaped tuning stub, resulting in a gain of 13.4 dB, was studied. The rectifier used a serial mounting diode and a microstrip sheet as a capacitor, which was essentially a DC bandpass filter, resulting in a high RF-to-DC conversion efficiency of the modified circuit of 80%. In practical operation, a maximum voltage of 18.5 V was achieved, along with a power conversion rate of up to 77.2% at 21 dBm of signal power when using 3.5-kΩ resistance. The gain is high, but the antenna structure is too large, i.e., 200 mm $\times$ 200 mm.

The authors of [35] introduced a monopolar antenna using triangular grooving techniques on the ground plane and an I-shaped reflector in implementing the air-gap technique. A gain of 8.36 dB was obtained. Combined with a full-wave rectifier circuit, this antenna could convert power at a conversion rate of up to 40% at 0 dBm at a maximum voltage of 0.46 V and convert voltage up to 6 V when using signal power up to 30 dBm. The antenna structure is not complicated, but has low gain.

In the method proposed in the present paper, a low signal power on the input power of −30.04 dB was used, transmitted at a distance of 1 m with a higher efficiency of 95.88%, as shown in Tab. 7.

Table 7: Comparison of rectenna efficiencies

Reference	Frequency (GHz)	Substrate	Antenna size (mm^3)	R (m)	Input power (dBm)	Gain (dB)	Efficiency (%)
[29]	2.45	RT/Duroid	$87 \times 80 \times 1.52$		−15	8.60	83
[30]	2.45	NPC-F260	$110 \times 110 \times 2.60$		0	6.70	63
[31]	2.45	FR4	$85 \times 100 \times 1.60$		20	7.13	78.70
[32]	2.37–2.52	FR4	$18 \times 30 \times 1.60$	1	5	5.60	68
[33]	2.45	Rogers	$228.60 \times 304.80 \times 1.524$	1	15	9.40	61
[34]	2.45	FR4	$200 \times 200 \times 3$		21	13.40	77.20
[35]	2.45	FR4	$100 \times 100 \times 1.60$	1	0	8.36	40
Present work	2.45	FR4	$120 \times 120 \times 1.60$	1	−30.04	11.62	95.88

6 Conclusions

The method for designing the structure and energy-harvesting circuit for an antenna proposed this research increased the antenna gain, reduced the complexity of the antenna structure, and obtained efficiency with a multiple voltage circuit. The antenna structure is a rectangular directional microstrip that is combined with an EBG mushroom-shaped magnetic frequency gap that can control the radiation direction and a 2×5 I-shaped metamaterial, placed at a distance of 10 mm. The gain increased from 7.21 to 11.67 dB with an efficiency of 39.76%. The entire antenna structure was constructed on a FR4 PCB with a constant electrical conductivity of 4.3 at 2.45 GHz in a Wi-Fi system. The energy was harvested with a rectifier circuit to convert the AC signal to DC and combined with an 8-times-multiplier voltage circuit that yielded voltages greater than those yielded by 6-, 10-, and 12-times-multiplier voltage circuits and increased the efficiency of the circuit by doubling the DC voltage 8 times. The optimum received energy was at an angle of 45° and a distance of 1 m. The obtained voltage was 2.82 mV, the current 0.34 mA, and the power 0.95 μW, with an efficiency of 95.88%. The proposed method is more efficient, the structure is not complicated, and less adjustment is needed.

Conflicts of Interest: The authors declare that they have no conflicts of interest to report regarding the present study.

References

[1] M. H. Nehrir, C. Wang, K. Strunz, H. Aki, R. Ramakumar *et al.,* "A review of hybrid renewable/alternative energy systems for electric power generation: Configurations, control, and applications," *IEEE Transactions on Sustainable Energy*, vol. 2, no. 4, pp. 392–403, 2011.

[2] T. H. Oh, S. Y. Pang and S. C. Chua, "Energy policy and alternative energy in Malaysia: Issues and challenges for sustainable growth," *Renewable and Sustainable Energy Reviews*, vol. 14, no. 4, pp. 1241–1252, 2010.

[3] P. McKendry, "Energy production from biomass (part 1): Overview of biomass," *Bioresource Technology*, vol. 83, no. 1, pp. 37–46, 2002.

[4] M. S. Dresselhaus and I. L. Thomas, "Alternative energy technologies," *Nature*, vol. 414, no. 6861, pp. 332–337, 2001.

[5] V. Devabhaktuni, M. Alam, S. S. S. R. Depuru, R. C. Green II, D. Nims *et al.,* "Solar energy: Trends and enabling technologies," *Renewable and Sustainable Energy Reviews*, vol. 19, no. 8, pp. 555–564, 2013.

[6] X. Lu, P. Wang, D. Niyato, D. I. Kim and Z. Han, "Wireless networks with RF energy harvesting: A contemporary survey," *IEEE Communications Surveys & Tutorials*, vol. 17, no. 2, pp. 757–789, 2014.

[7] M. Piñuela, P. D. Mitcheson and S. Lucyszyn, "Ambient RF energy harvesting in urban and semi-urban environments," *IEEE Transactions on Microwave Theory and Techniques*, vol. 61, no. 7, pp. 2715–2726, 2013.

[8] F. Iwanda, Z. Zulfi and Y. Wahyu, "Rectifying antenna (rectenna) untuk sinyal tv uhf 470–806 Mhz," *eProceedings of Engineering*, vol. 5, no. 3, pp. 5483–5490, 2018.

[9] R. K. Sidhu, J. S. Ubhi and A. Aggarwal, "A survey study of different RF energy sources for RF energy harvesting," in *Int. Conf. on Automation, Computational and Technology Management*, Amity University, London, United Kingdom, pp. 530–533, 2019.

[10] M. Hasan, M. Rahman, M. R. I. Faruque, M. T. Islam and M. U. Khandaker, "Electrically compact SRR-loaded metamaterial inspired quad band antenna for bluetooth/WiFi/WLAN/WiMAX system," *Electronics*, vol. 8, no. 7, pp. 790, 2019.

[11] C. A. Balanis, "Antenna theory and design," NY, USA: John Willey & Sons, 1997.

[12] W. Naktong, P. Boonmaitree, S. Kornsing, E. Khoomwong and A. Ruengwaree, "CPW-fed rectangular aperture antenna with two-step ground-plane tuning for UWB applications," *RMUTI Journal Science and Technology*, vol. 7, no. 2, pp. 50–66, 2014.

[13] W. Naktong, N. Fhafhiem, A. Innok and A. Ruengwaree, "Study of rectanna using directive antenna at frequency of 2.45 GHz," in *10th South East Asian Technical University Consortium Symp.*, Tokyo, Japan, 2016.

[14] E. K. I. Hamad and A. Abdelaziz, "Metamaterial superstrate microstrip patch antenna for 5G wireless communication based on the theory of characteristic modes," *Journal of Electrical Engineering*, vol. 70, no. 3, pp. 187–197, 2019.

[15] A. Lalbakhsh, M. U. Afzal, K. P. Esselle, S. L. Smith and B. A. Zeb, "Single-dielectric wideband partially reflecting surface with variable reflection components for realization of a compact high-gain resonant cavity antenna," *IEEE Transactions on Antennas and Propagation*, vol. 67, no. 3, pp. 1916–1921, 2019.

[16] B. A. Munk, "Frequency selective surfaces: Theory and design," NY, USA: John Wiley & Sons, 2005.

[17] S. Luo, Y. Li, Y. Xia and L. Zhang, "A low mutual coupling antenna array with gain enhancement using metamaterial loading and neutralization line structure," *Applied Computational Electromagnetics Society Journal*, vol. 34, no. 3, pp. 411–419, 2019.

[18] H. Ö. Yılmaz and F. Yaman, "Meta-material antenna designs for a 5.8 GHz doppler radar," *IEEE Transactions on Instrumentation and Measurement*, vol. 69, no. 4, pp. 1775–1782, 2019.

[19] M. E. Atrash, M. A. Abdalla and H. M. Elhennawy, "A wearable dual-band low profile high gain low SAR antenna AMC-backed for WBAN applications," *IEEE Transactions on Antennas and Propagation*, vol. 67, no. 10, pp. 6378–6388, 2019.

[20] P. K. T. Rajanna, K. Rudramuni and K. Kandasamy, "A high-gain circularly polarized antenna using zero-index metamaterial," *IEEE Antennas and Wireless Propagation Letters*, vol. 18, no. 6, pp. 1129–1133, 2019.

[21] B. Hasan and K. Raza, "Dual band slotted printed circular patch antenna with superstrate and EBG structure for 5G applications," *Mehran University Research Journal of Engineering and Technology*, vol. 38, no. 1, pp. 227–238, 2019.

[22] W. Brown, J. Mims and N. Heenan, "An experimental microwave-powered helicopter," in *1958 IRE Int. Convention Record*, New York, NY, USA, pp. 225–235, 1966.

[23] Q. Chen and H. Zhang, "High-gain circularly polarized fabry-pérot patch array antenna with wideband low-radar-cross-section property," *IEEE Access*, vol. 7, pp. 8885–8889, 2019.

[24] X. Jiang, F. Jia, Y. Cao, P. Huang, J. Yu *et al.,* "Ka-band 8×8 low-sidelobe slot antenna array using a 1-to-64 high-efficiency network designed by new printed RGW technology," *IEEE Antennas and Wireless Propagation Letters*, vol. 18, no. 6, pp. 1248–1252, 2019.

[25] J. Khan, D. A. Sehrai, M. A. Khan, H. A. Khan, S. Ahmad *et al.,* "Design and performance comparison of rotated y-shaped antenna using different metamaterial surfaces for 5G mobile devices," *Computers, Materials & Continua*, vol. 60, no. 2, pp. 409–420, 2019.

[26] D. A. Sehrai, F. Muhammad, S. H. Kiani, Z. H. Abbas, M. Tufail *et al.,* "Gain-enhanced metamaterial based antenna for 5G communication standards," *Computers, Materials & Continua*, vol. 64, no. 3, pp. 1587–1599, 2020.

[27] S. H. Kiani, A. Altaf, M. Abdullah, F. Muhammad, N. Shoaib *et al.,* "Eight element side edged framed MIMO antenna array for future 5G smartphones," *Micromachines*, vol. 11, no. 11, pp. 1–13, 2020.

[28] E. A. Kadir, A. P. Hu, M. Biglari-Abhari and K. C. Aw, "Indoor WiFi energy harvester with multiple antenna for low-power wireless applications," in *2014 IEEE 23rd Int. Symp. on Industrial Electronics*, Istanbul, Turkey, pp. 526–530, 2014.

[29] H. Sun, Y. X. Guo, M. He and Z. Zhong, "Design of a high-efficiency 2.45-GHz rectenna for low-input-power energy harvesting," *IEEE Antennas and Wireless Propagation Letters*, vol. 11, pp. 929–932, 2012.

[30] Y. Huang, N. Shinohara and H. Toromura, "A wideband rectenna for 2.4 GHz-band RF energy harvesting," in *IEEE Wireless Power Transfer*, Aveiro, Portugal, pp. 1–3, 2016.

[31] S. Ahmed, Z. Zakaria, M. N. Husain and A. Alhegazi, "Design of rectifying circuit and harmonic suppression antenna for RF energy harvesting," *Journal of Telecommunication, Electronic and Computer Engineering*, vol. 9, no. 2–13, pp. 63–67, 2017.

[32] Q. Awais, Y. Jin, H. T. Chattha, M. Jamil, H. Qiang *et al.,* "A compact rectenna system with high conversion efficiency for wireless energy harvesting," *Journal of Telecommunication, Electronic and Computer Engineering*, vol. 9, no. 2–13, pp. 63–67, 2017.

[33] F. Erkmen, T. S. Almoneef and O. M. Ramahi, "Scalable electromagnetic energy harvesting using frequency-selective surfaces," *IEEE Transactions on Microwave Theory and Techniques*, vol. 6, no. 5, pp. 2433–2441, 2018.

[34] X. Li, L. Yang and L. Huang, "Novel design of 2.45-GHz rectenna element and array for wireless power transmission," *IEEE Access*, vol. 7, pp. 28356–28362, 2019.

[35] M. A. M. Said, Z. Zakaria, M. N. Husain, M. H. Misran and F. S. M. Noor, "2.45 GHz rectenna with high gain for RF energy harvesting," *Telkomnika*, vol. 17, no. 1, pp. 384–391, 2019.

[36] S. Ahmed, M. N. Husain, Z. Zakaria, M. S. I. M. Zin and A. Alhegazi, "Rectenna designs for RF energy harvesting system: A review," *International Journal on Communications Antenna and Propagation*, vol. 6, no. 2, pp. 82–91, 2016.

[37] W. Hong, Y. Cao, L. Deng, S. Li, M. Li *et al.,* "A circular polarized rectenna with out-of-band suppression for microwave power transmission," *International Journal of Antennas and Propagation*, vol. 2016, pp. 1–7, 2016.

[38] N. Fhafhiem, P. Krachodnok and R. Wongsan, "Curved strip dipole antenna on EBG reflector plane for RFID applications," *Wseas Transactions on Communications*, vol. 9, pp. 374–383, 2010.